COMPONENT PART NOTICE

THIS PAPER IS A COMPONENT PART OF THE FOLLOWING COMPILATION REPORT:

TITLE: Proceedings of the Antenna Applications Symposium Held at Urbana, Illinois on 19-21 September 1984. Volume 2.

TO ORDER THE COMPLETE COMPILATION REPORT, USE AD-A153 258.

THE COMPONENT PART IS PROVIDED HERE TO ALLOW USERS ACCESS TO INDIVIDUALLY AUTHORED SECTIONS OF PROCEEDING, ANNALS, SYMPOSIA, ETC. HOWEVER, THE COMPONENT SHOULD BE CONSIDERED WITHIN THE CONTEXT OF THE OVERALL COMPILATION REPORT AND NOT AS A STAND-ALONE TECHNICAL REPORT.

THE FOLLOWING COMPONENT PART NUMBERS COMPRISE THE COMPILATION REPORT:

AD#: AD-P004 620 thru AD#: AD-P004 637

AD#: AD#:

AD#: AD#:

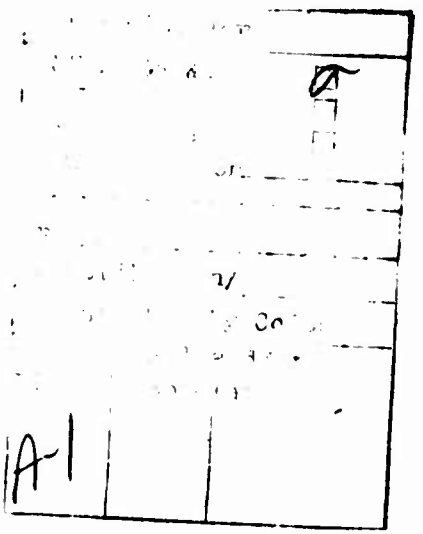

DTIC FORM 463 MAR 85

OPI: DTIC-TID

Design and Error Analysis for the WR10 Thermal Noise Standard

William C. Daywitt
Electromagnetic Fields Division
National Bureau of Standards
Boulder, Colorado 80303

Abstract

This note describes the design and error analysis of a WR10 thermal noise power standard. The standard is designed to operate at the boiling point of liquid nitrogen with a noise temperature accurate to ± 1 K.

Key words: antenna efficiency; diffraction; error analysis; millimeter wave; noise standard; plane-wave scattering matrix.

1. Introduction

Over the past twenty years, the Electromagnetic Fields Division of the National Bureau of Standards (NBS) has built a number of coaxial and waveguide noise sources[1-3] consisting of single-mode, uniform transmission lines terminated in reflectionless loads. The accuracy of their calculated noise temperatures are typically 1% which tends to degrade as the operating frequency increases. The basic design is illustrated in figure 1 where the termination and a portion of the transmission line are immersed in a thermal reservoir at temperature T_m, with the

remaining portion of the line leading to the output connector at room temperature T_0. The temperature distribution T_x of the line is also illustrated where the room-temperature portion of the line has a length ℓ. Radiation from the termination and the dissipative losses of the line result in a noise temperature

$$T_n = T_m + \Delta T \tag{1}$$

where, for the idealized distribution shown,

$$\Delta T \doteq (2a'\ell)\ (T_0 - T_m). \tag{2}$$

The attenuation coefficient a' refers to the line at T_0, and the equations indicate that only that portion of the line contributes to the excess (in excess of thermal equilibrium conditions) noise temperature ΔT.

The largest source of error in calculating the noise temperature by eq (1) is the attenuation $2a'\ell$, which is usually estimated to an error varying from 10% to 20%. With this large an error, it is necessary to keep the attenuation small (to maintain the error in T_n less than 1%), implying either a small attenuation coefficient a', a short transition length ℓ, or both. In the microwave frequency range and below, the attenuation can be kept down with relatively simple engineering designs; but as the

frequency increases into the millimeter-wave range, this becomes more of a problem[3]. In this higher frequency range, surface roughness also plays a bigger role[4], causing an additional increase in the attenuation.

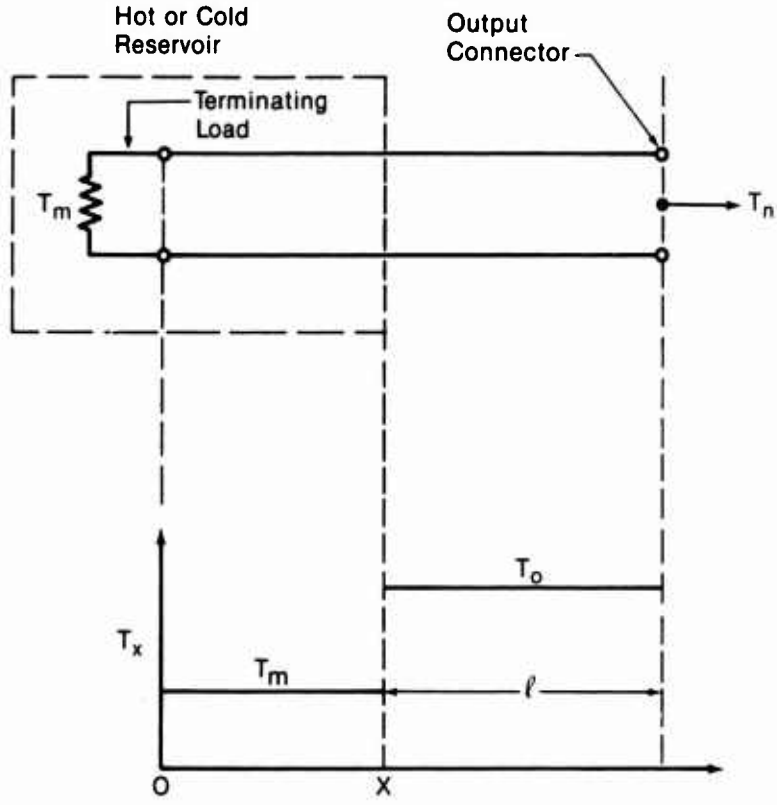

Figure 1. Schematic diagram of a transmission-line type noise standard.

To circumvent the engineering difficulties, it was decided to abandon the transmission-line type of noise standard in favor of a

design incorporating a millimeter-wave horn antenna "looking" at an absorber of known temperature. The resulting antenna noise temperature is close to the measured temperature T_m of the absorber, with additional noise contributions from the dissipative antenna losses, and from the antenna side and back lobes. This type of noise source is not new, but its use as a primary reference standard of high accuracy required the successful resolution of two previously unanswered questions: can a useful expression for the noise efficiency (defined in next section) of the antenna with sources in its radiating near field[5] be found; and can the error caused by near-field excess radiation (in excess of thermal-equilibrium conditions) entering the side and back lobes of the antenna be estimated?

The antenna noise efficiency derivation described in the next section and in a previous note[6] is based upon the plane-wave scattering-matrix (PWSM) theory of antennas[7]. This efficiency, because of reciprocity, reduces to the antenna radiation efficiency. However, in contrast to the usual definition[8] of the radiation efficiency, the PWSM description reveals enough of the structure of the efficiency to permit a detailed calculation and error analysis of its magnitude. The PWSM formalism is used solely to derive an expression for the antenna noise efficiency and excess noise temperature with the cavity in the antenna

radiating near field, and to show how the efficiency can be evaluated in terms of antenna far-field quantities.

Insights gleaned from the Uniform Theory of Diffraction (UTD)[9] are used[6] to eliminate the angle-dependent components of the noise efficiency. The error incurred from neglecting these contributions to the efficiency is then estimated. The residual, angle-independent part of the efficiency is estimated[6] by substituting the rectangular waveguide expression for the absorption coefficient, changing the cross-sectional dimensions to conform to the interior dimensions of the horn antenna. The waveguide expression is used because of the nonexistence of pyramidal horn mode equations. An estimate of the error caused by this substitution is also made[6].

Effects of surface roughness on dissipative loss are reviewed[6], and an attempt is made to clarify some disagreements found in the literature[10,11]. A modified expression for the corresponding noise efficiency is then determined.

Due to more intense fields in the waveguide portion of the horn, dissipative loss is greater there than in the horn flare. Consequently, the horn waveguide lead is made as short as possible without introducing a significant amount of higher-mode contamination in the antenna noise temperature. The minimum allowable length is determined[6] along with an estimate of the error due to these higher modes.

The UTD is used[6] to estimate the noise temperature error due to the cavity wall temperature being greater than the temperature of the absorber, and to estimate the effect of multiple reflections between the horn and rear cavity wall. An upper limit to the magnitude of the excess cavity noise is determined, and (by examining multiple reflections between the horn aperture and rear cavity wall) separating the total excess noise into a sum of excess antenna and cavity noises is justified.

2. Antenna noise efficiency and construction of the horn

The antenna noise temperature T_n is determined from eq (1) with a different excess noise temperature ΔT than that given in eq (2) for transmission-line type noise standards. This new correction temperature has the form

$$\Delta T = (1 - \alpha)\ (T_0 - T_m) \qquad (3)$$

for an antenna inside a reflectionless, isothermal cavity. α is the noise efficiency, T_0 is the physical temperature of the antenna, and T_m is the physical temperature of the cavity. An equation for the efficiency, when the cavity is in the radiating near field of the antenna, is derived by use of the antenna scattering matrix[6] and the Clausius statement of the second law of thermodynamics[12]. The details of the derivation reveal that the

cavity walls need not be strictly reflectionless, only that no multiple reflections take place between the cavity and the antenna (an important distinction that is utilized in constructing the standard).

One interesting and useful feature that comes from the derivation is that the efficiency is the same whether the radiating sources (the cavity) are in the antenna near or far field. This result allows the efficiency to be more easily examined with far-field quantities. The result is

$$\alpha = \frac{1}{\Omega_a} \int \left| \frac{r\underline{E}'(\underline{r})}{r\underline{E}(\underline{r})} \right|^2 P_n(\Omega) d\Omega \qquad (4)$$

In eq (4), Ω_a is the antenna solid angle, $\underline{r}$ is the radius vector from the antenna aperture to the far-field point (r is the magnitude), $P_n(\Omega)$ is the normalized power pattern where Ω stands for the antenna pointing angles, $d\Omega$ is the differential solid angle, and $r\underline{E}(\underline{r})$ is the E-field pattern. The prime refers to the real (lossy) antenna, the unprimed quantities belonging to the same antenna with no losses.

Ideally, the pattern ratio in eq (4) could be measured, or calculated from Maxwell's equations, but the measurement is too inaccurate to be useful and the calculation is prohibitively

difficult. However, since most of the loss comes from the waveguide and flare portions of the horn[6], the efficiency is easily calculated if losses from the remainder of the horn are neglected. Figure 2 shows an isometric view of the horn designed for the WR10 frequency band (75 GHz to 110 GHz) to take advantage of this situation. Reflections from the waveguide-flare junction,

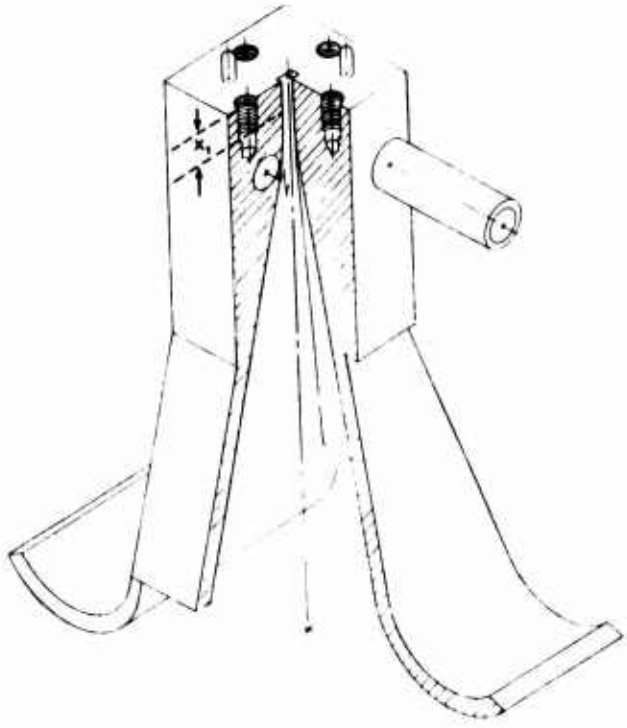

Figure 2. Isometric view of the WR10 horn antenna.

or throat, are minimized by joining the waveguide and flare with a circular arc of sufficiently large radius[13], beginning at x_1 and ending tangentially on the flared walls. A quarter-round (3 wavelength radius) matching section[14] at the aperture, in addition to a large aperture cross section[15], minimize the aperture reflections. With multiple reflections interior to the horn eliminated, a wave entering the horn flare from the waveguide maintains its TE_{10}-mode configuration out to the aperture.

Before including the throat taper and the aperture matching section into the design, and after choosing the E-plane aperture dimension, Braun's equations[16] were used to determine the other aperture dimension and the flare angles and lengths to insure approximately equal E- and H-plane beam widths and a simple butt joint at the waveguide-flare junction. The waveguide length x_1 was chosen[6] to minimize the effects of higher modes (generated by radiation incident on the antenna from the cavity) on the antenna noise temperature. Finally, a water jacket was included around the waveguide-throat region to maintain this high-loss area at a constant known temperature.

The calculated horn attenuation neglects the effect of surface roughness on the losses, predicting a loss that is less than the actual value. For an isotropically rough surface, the horn attenuation coefficient increases by a factor K, which is independent of position inside the horn--depending only upon the

roughness of the surface and the operating frequency. Furthermore, it is reasonable to assume that K is independent of temperature. These considerations imply that K can be determined by comparing the measured and calculated (assuming no surface roughness) attenuation for a waveguide section with the same surface roughness as the horn. A picture of the horn with the four waveguide sections and quarter-wave short (94.5 GHz) used to determine K is shown in figure 3. The horn was constructed by machining a stainless-steel mandril to the interior horn dimensions, flashing it with gold, and electroforming copper on top of the gold. After

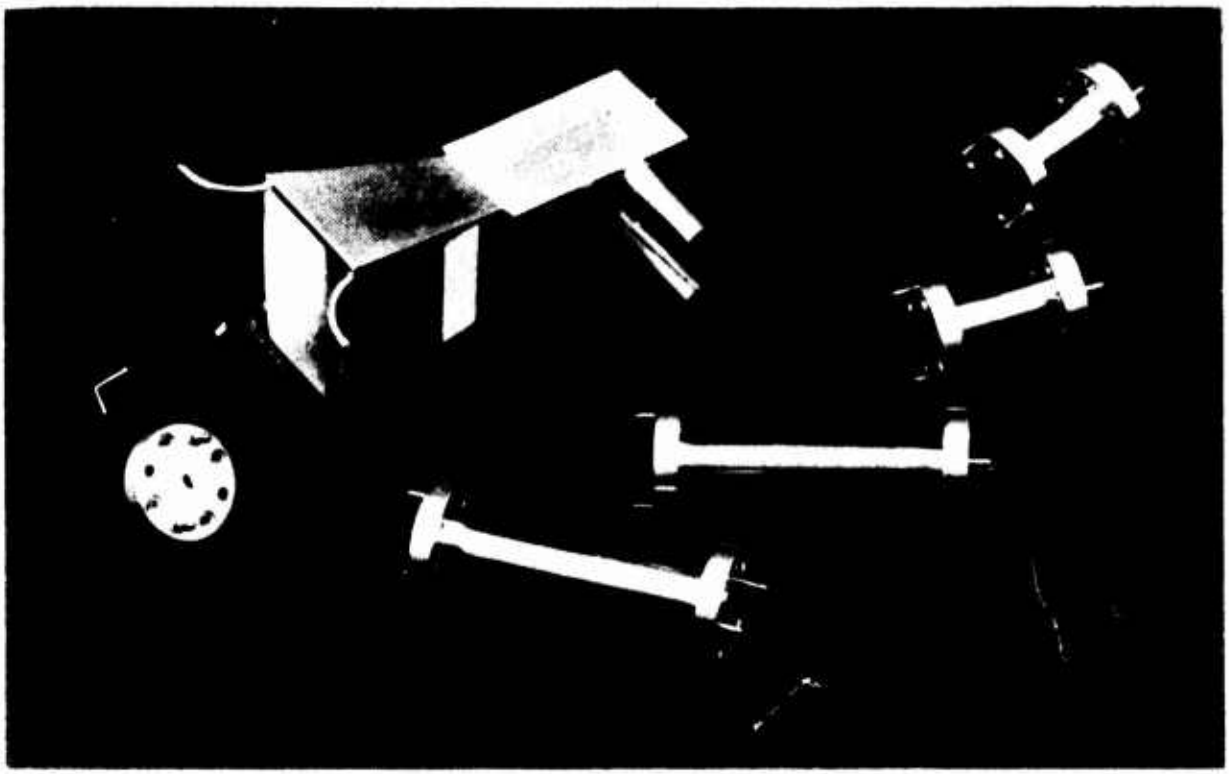

Figure 3. WR10 horn antenna, waveguide sections, and quarter-wave short.

electroforming and machining, the mandril was removed, leaving the horn shown in the figure. The process was repeated to produce the four waveguide sections with the same interior surface roughness as the horn. Then, after determining K for the waveguide section, the efficiency of the horn was calculated from

$$\alpha = e^{-2K\int a' dz} \qquad (5)$$

where the attenuation coefficient a' is a function of the dimensions and temperature of the horn at position z along the horn axis[6]. The integral is performed over the length of the horn.

Figures 4, 5, and 6 show the results of the calculations with K = 1. The attenuation coefficient a' for 75 GHz and 110 GHz is plotted as a function of z along the horn axis, with the waveguide flange of the horn at the origin. The waveguide portion of the horn extends from z = 0 to z = 0.31, where the transition to the flare starts. The aperture and the beginning of the quarter-round matching sections are at z = 7.0, and the water jacket extends from the flange to z = 3.6. Figure 5 shows the total horn attenuation (the exponent of eq (5) with K = 1) as a function of frequency, leading to the excess noise temperature shown in figure 6.

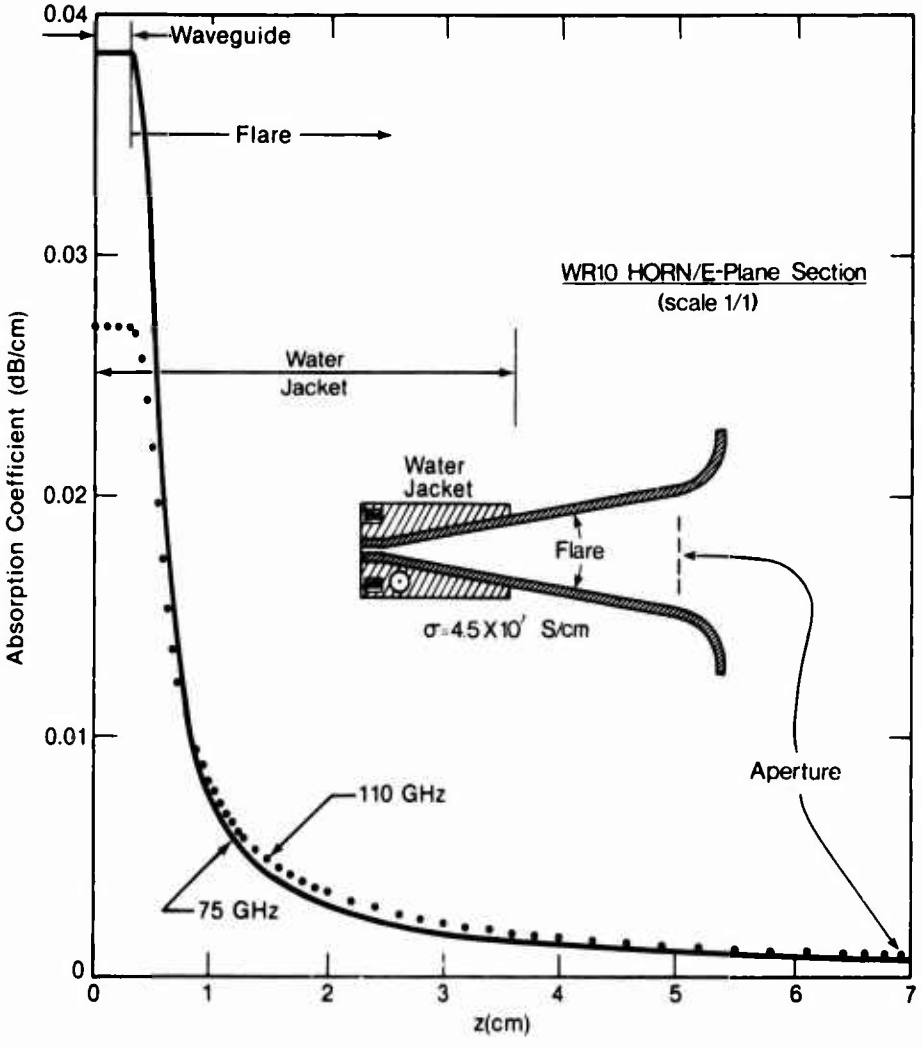

Figure 4. Attenuation coefficient for the WR10 horn antenna.

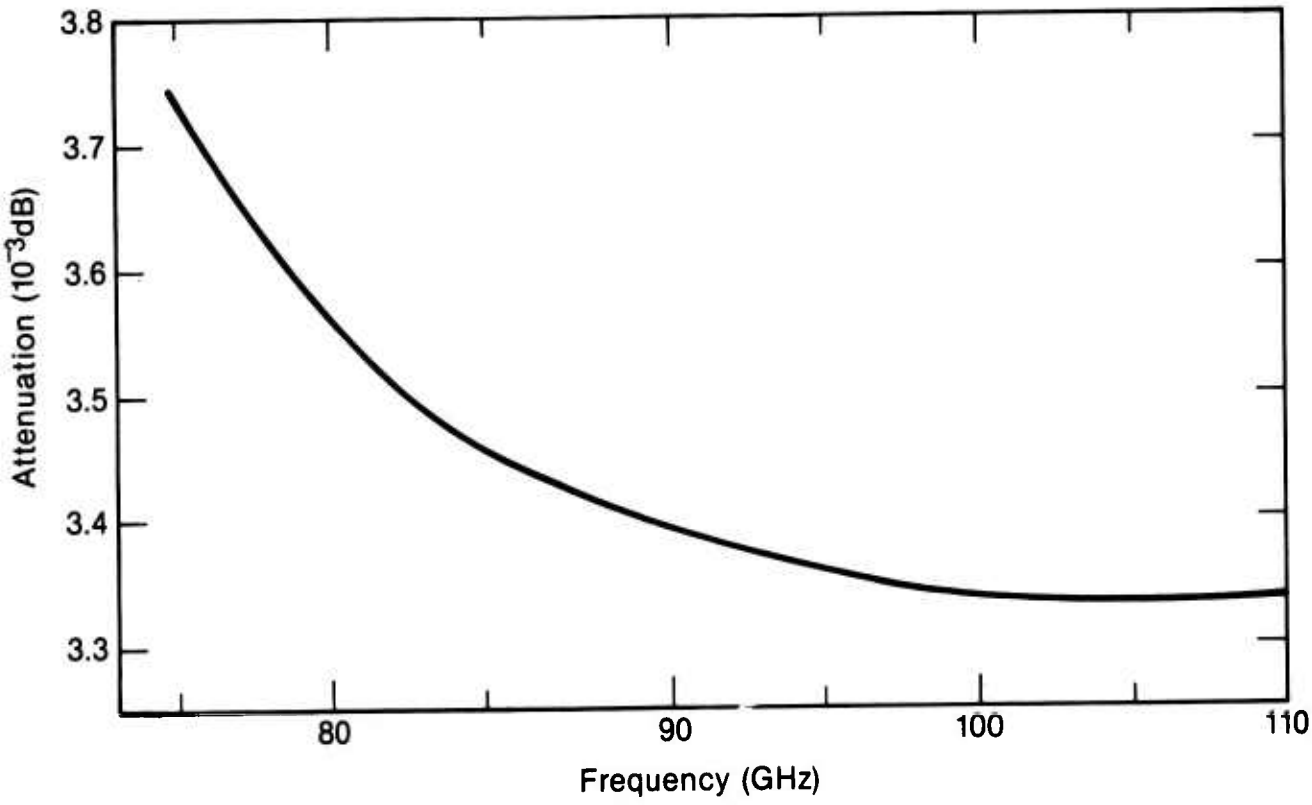

Figure 5. Attenuation versus frequency for the waveguide, throat, and flare portions of the WR10 horn antenna.

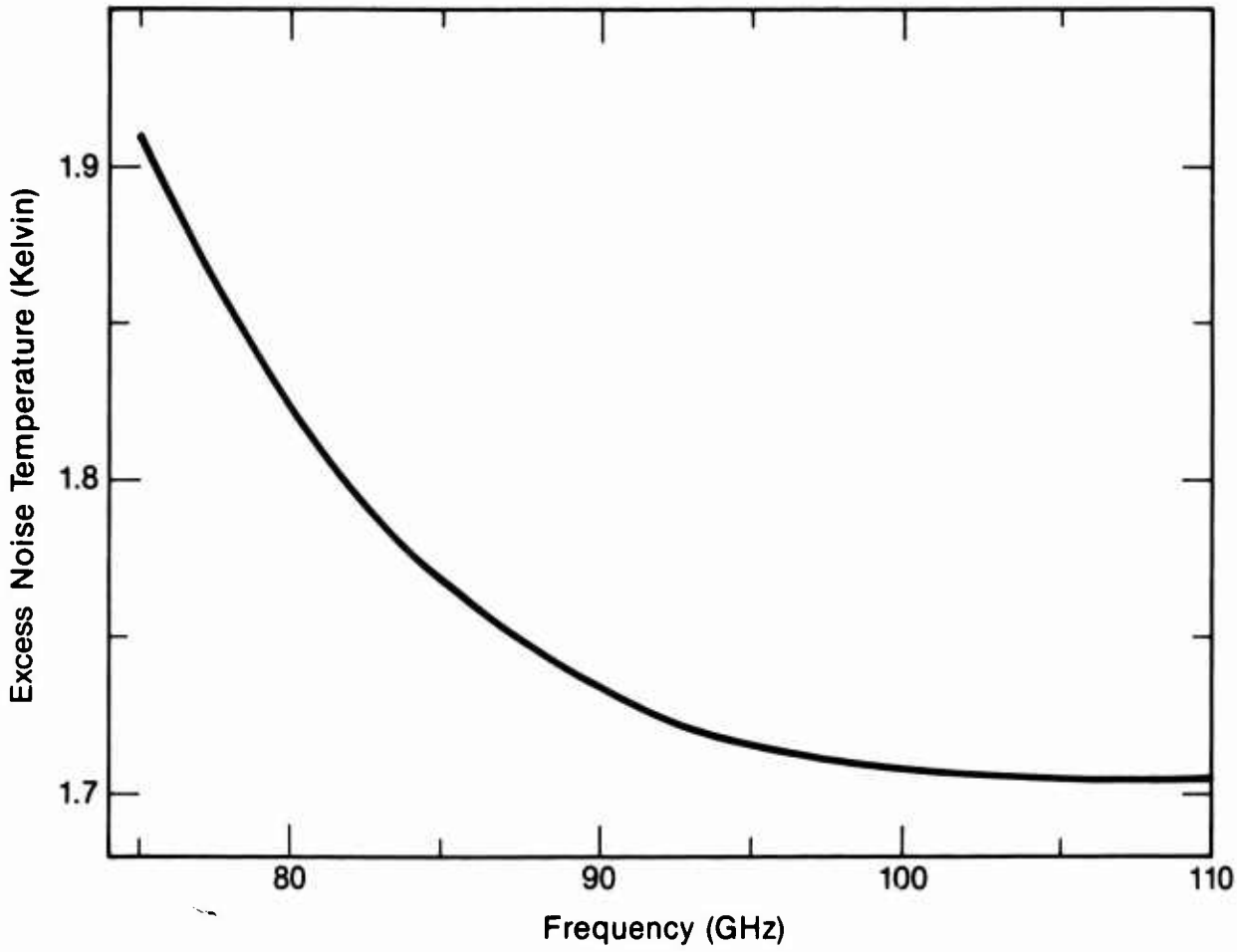

Figure 6. Correction noise temperature for the WR10 noise standard.

3. Construction and operation of the cavity

An assembly drawing of the WR10 noise standard is shown in figure 7. The horn antenna is suspended at the top of the cavity by a yoke (items 18A and 18B) that attaches it to a flexible, beryllium-copper membrane (17) which fits loosely in a holder (7) that allows approximately 8 mm side motion. This motion, with the flexibility of the membrane, permits the horn waveguide flange to be connected to a radiometer without supporting the weight of the entire standard, greatly reducing problems associated with flange misalignment. The cavity consists of the yoke and membrane, the silicon-carbide absorber (13), and the load holder (14). The inside cavity walls are polished and gold flashed to reduce thermal radiation from their surfaces. Two radiation shields (6C, 6E) help reduce the amount of external radiation entering the cavity. The bottom portion of the cavity is immersed in liquid nitrogen, allowing the liquid to leak through the bottom of the holder and be absorbed by the silicon carbide. The liquid level is maintained between the maximum and minimum levels shown in the figure. Millimeter-wave absorber (16) is inserted between the bottom of the load holder and the vacuum flask (12) to absorb radiation entering the flask from outside the standard. By using this absorber, the radiation temperature[17] of the radiation entering the cavity from the flask area is reduced from

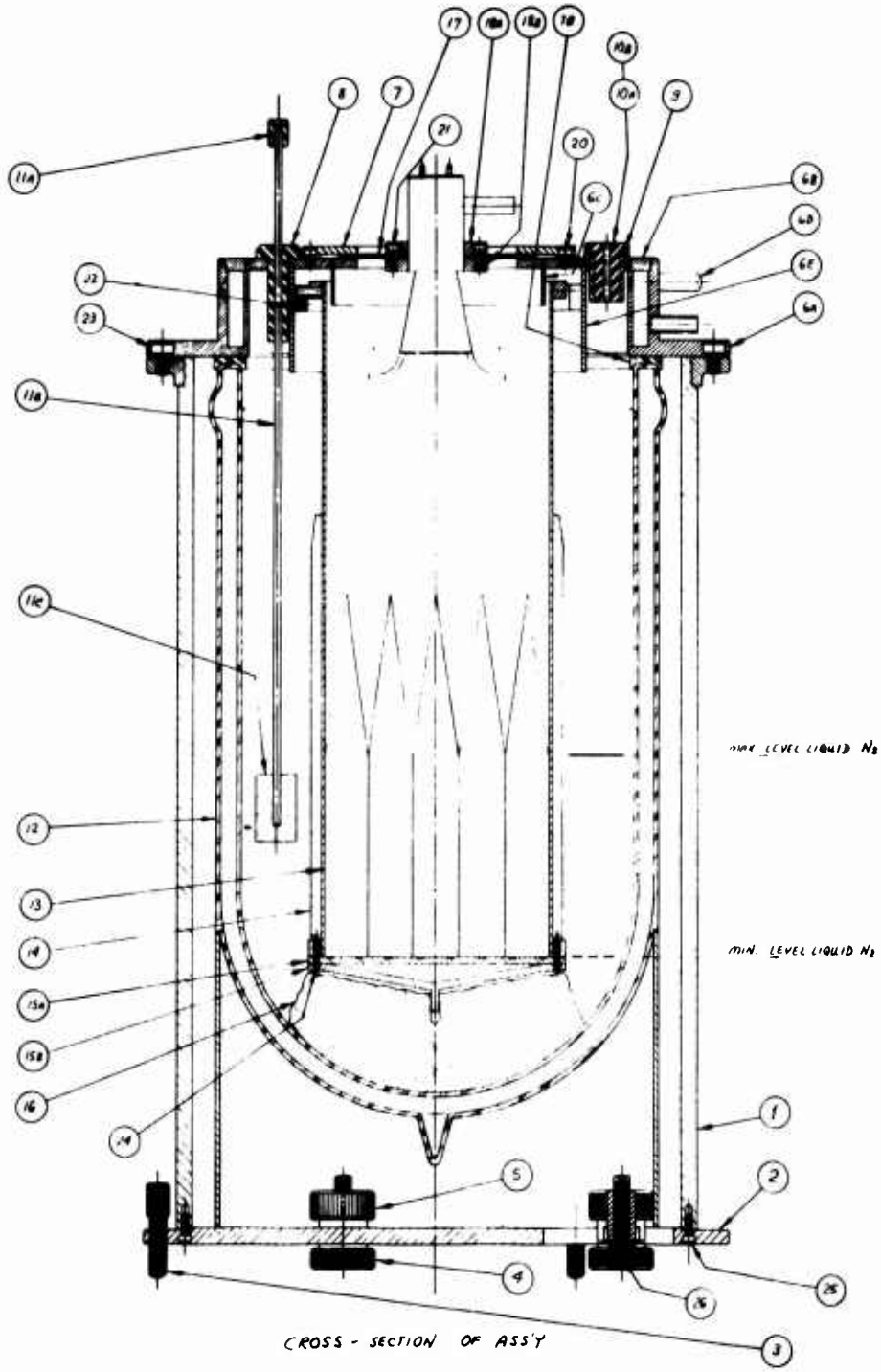

Figure 7. Assembly drawing of the WR10 noise standard.

approximately 300 K to 2 K above the boiling temperature (77 K) of the liquid. Once the flask is filled to the maximum level, it takes approximately seven hours for the liquid to boil down to the minimum usable level. Figure 8 is a photograph of the completed assembly.

The silicon-carbide absorber was manufactured from commercially available grinding-wheel stock (grad P, grit C320, vitrified bond, silicon carbide) by cutting the stock into rectangular shapes and sharpening the ends. The pieces were then fastened together and the assembly ground to form the cylindrical shape shown in figure 9. When inserted in the holder (fig. 10), the cohesive action between the silicon-carbide particles and the liquid nitrogen draws the liquid up into the wedges, allowing the liquid to boil off on the wedge surfaces. With this technique, the temperature of the radiating surface of the absorber is maintained at the boil-off temperature of the liquid nitrogen to within 0.2 K, independent of the level of the liquid in the flask.

4. Results, errors, and conclusions

Equations (1), (3), and (5) are used to calculate the noise temperature T_n of the standard, where T_m is the measured temperature (liquid nitrogen boil-off temperature) of the absorber, T_o is the temperature of the horn antenna (room temperature), α is the noise efficiency of the horn, K is the

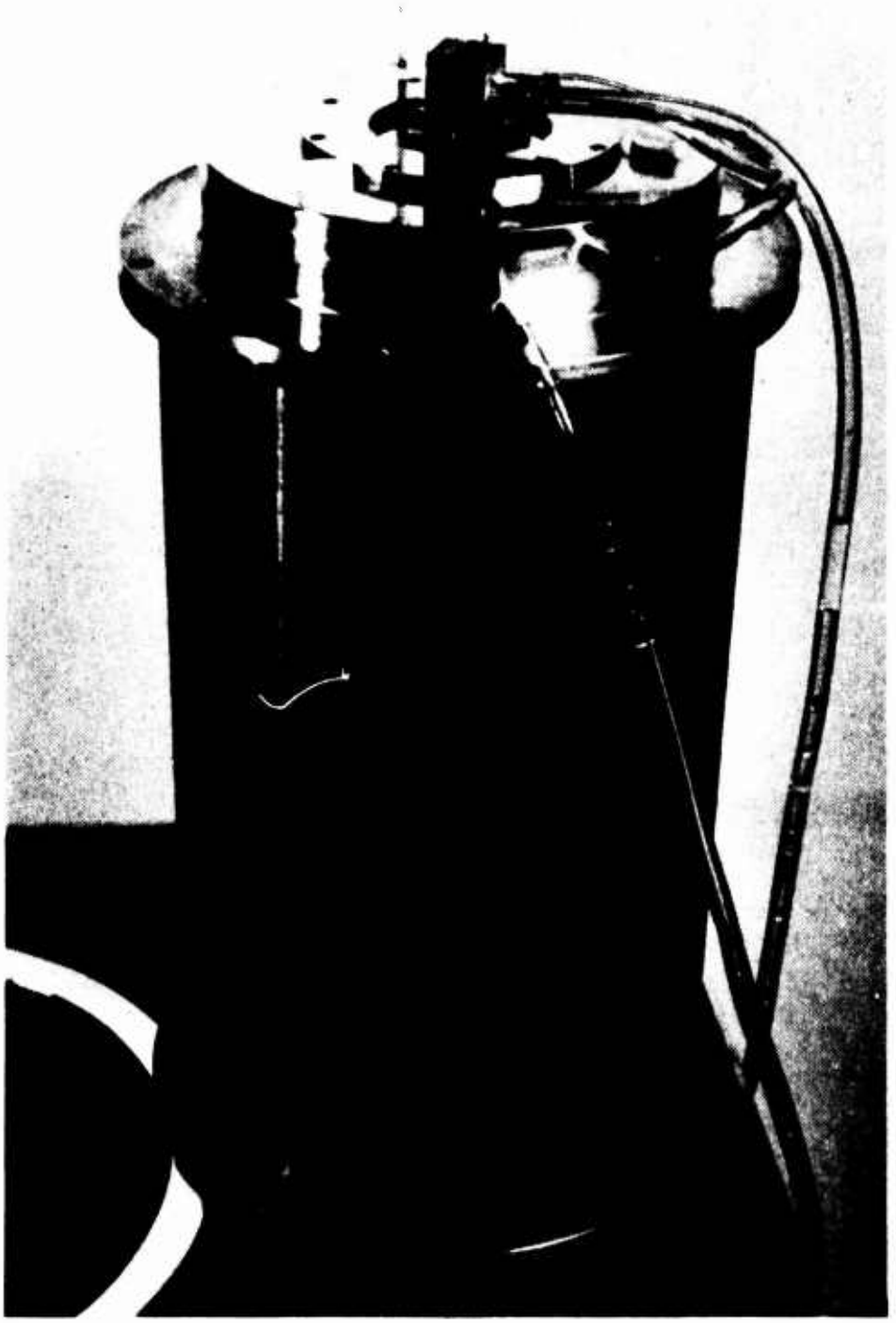

Figure 8. WR10 noise standard.

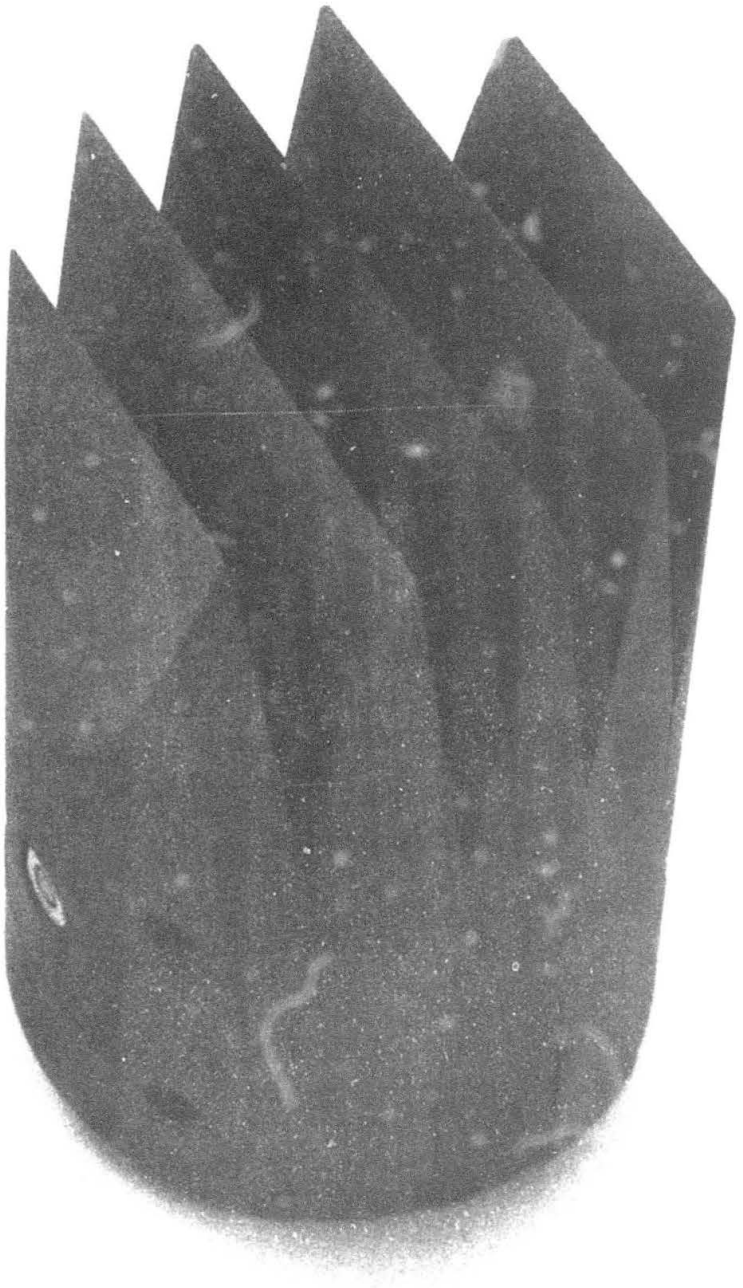

Figure 9. Silicon-carbide absorber.

roughness factor, and a' is the absorption coefficient at position z along the horn axis. Six possible sources of error accompany the use of these equations: (i) higher-mode contamination of the noise temperature, (ii) multiple reflections between the horn and rear cavity wall, (iii) wall temperatures greater than the absorber temperature, (iv) uncertainty in T_m, (v) uncertainty in T_o, and (vi) uncertainties in the noise efficiency. These sources of error are discussed below and summarized in table 1 along with the resulting errors they produce in the output noise temperature.

The length of the waveguide portion of the horn was chosen to adequately filter out the higher waveguide modes generated in the horn flare by radiation from the cavity incident on the horn. The calculations[6] show, that for 0.31 cm, the residual contamination amounts to no more than + 0.12% of the noise temperature.

Multiple reflections between the back wall of the cavity and the horn affect both the validity and magnitude of the correction noise temperature in eq (3). Calculations[6] show the discrepancy in the magnitude to be insignificant, indicating that the assumption of a reflectionless cavity in the derivation of eq (3) leads to no larger an error than - 0.05%.

The temperature of the cavity back and side walls varies from room temperature at the top of the cavity (fig. 7) to liquid-nitrogen temperature where the side wall meets the absorber. The elevated wall temperatures cause the noise temperature to be in

excess of the load temperature T_m. The resulting error[6] is no larger than - 0.10%.

The temperature of the absorber wedges was found to be within 0.1 K (the experimental error) of the liquid-nitrogen boil-off temperature (which was measured with the same thermocouple). When the standard is in use, the absorber temperature is determined by reading the atmospheric pressure (± 1 mm Hg) off a precision barometer and converting to the boil-off temperature (± 0.14 K) via standard vapor-pressure equations[18]. Care was taken in constructing the standard to insure a positive flux of nitrogen boil-off gas from the enclosure, preventing contamination of the liquid nitrogen by atmospheric gasses, and allowing the equations to be used to an assumed accuracy of 0.02 K. The total error (0.26 K) in measuring the absorber temperature is the sum of these three errors. This causes an error of less than 0.34% in the noise temperature.

The temperature of the horn, reduced slightly by cooling from the liquid-nitrogen boil-off gas, is determined by circulating room-temperature water through the water jacket (fig. 2). The water temperature is measured before entering the horn by use of a precision (± 1 K) mercury thermometer, and the temperature of the high-loss portions of the horn is depressed no more than 1 K by the boil-off gas. The horn temperature error is, therefore, no

Table 1. Errors in the WR10 (75 GHz - 110 GHz) noise standard

Source of Error	Source Uncertainty	Resulting Percentage Error in T_n
1. Higher modes	---	0
2. Multiple reflections between horn & cavity	---	$^{+0}_{-0.05}$
3. Elevated cavity-wall temperature	---	$^{+0}_{-0.10}$
4. Uncertainty in T_m	± 0.26 K	± 0.34
5. Uncertainty in T_0	± 2 K	± 0.02
6. Uncertainties in α		
6.1 Neglecting losses beyond aperture	---	$^{+0}_{-0.01}$
6.2 Using waveguide loss equation	---	± 0.01
6.3 Dimensional uncertainties	± 0.0025 cm	± 0.06
6.4 Uncertainties in dc resistivity curve	± 5%	± 0.01
6.5 Uncertainties in K	± 5%	± 0.06
Total error (linear sum)		$^{+0.5\ \%}_{-0.7\ \%}$

larger than 2 K, causing an error of less than 0.02% in the noise temperature.

Errors in the noise efficiency fall into two classes: errors due to the approximations leading to eq (5), and errors due to uncertainties in the parameters used in the equation. The first class contains an error due to neglecting dissipative horn losses beyond the aperture[6], resulting in a noise temperature error less than a negative 0.01%; and an error due to the nonexistence of equations describing pyramidal horn fields[6] resulting in an error no larger than 0.01%. The parametric errors are due to uncertainties (± 0.0025 cm) in the internal horn dimensions, in the slope versus temperature curve for the dc resistivity of the horn walls (± 5%), and in the roughness factor K. The first two result in noise-temperature errors of less than 0.01% and 0.06%, respectively.

The roughness factor at 297 K was determined by comparing the measured and calculated values of attenuation for the waveguide sections shown in figure 3. Errors in the roughness factor are due to errors (± 0.0012 cm) in the measured dimensions of the waveguide sections, and uncertainties associated with the six-port millimeter-wave system[19] used to measure the attenuation. The roughness factor was determined to be 1.14 (± 0.05) at 94.5 GHz, with an error no larger than 0.06% in the noise temperature.

The sum of errors in table 1 for the noise-temperature output of the noise standard is within 1%, showing that it is possible to construct a precision horn/absorber type of standard, and, thus, eliminate the engineering problems mentioned in the introduction. Furthermore, this type of standard can be easily duplicated at the higher millimeter-wave bands.

Calculations using the UTD show that, if the yoke and membrane (items 17, 18A, and 18B in fig. 7) are removed from the standard, the noise temperature increases by approximately 0.7%. If, in addition, the aperture-matching quarter-rounds (the curved sections on the horn aperture in fig. 2) are removed from the horn, this figure increases from 0.7% to approximately 3%. Therefore, the yoke and membrane are needed to insure an accurately known noise temperature.

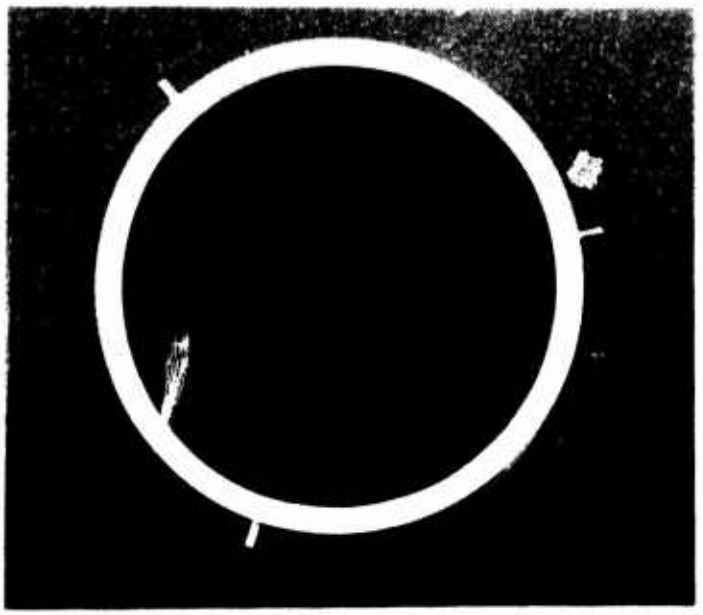

Figure 10. Top view of the cavity.

5. Acknowledgments

The author takes great pleasure in acknowledging the many beneficial contributions from his colleagues in the Electromagnetic Fields Division who unhesitatingly shared their expertise in a number of seminars and many private discussions.

6. References

1. Arthur, M. G.; Driver, L. D. A precision HF-noise power measurement system. ISA Transactions, 10: 264 - 268; 1971.

2. Wells, J. S.; Daywitt, W. C.; Miller, C. K. S. Measurement of effective temperature of microwave noise sources. IEEE Trans. on I&M, IM-13: 17 - 28; 1964 March.

3. Daywitt, W. C. WR15 thermal noise standard. Nat. Bur. Stand. (U.S.) Tech. Note 615; 1972 March.

4. Tischer, F. J. Experimental attenuation of rectangular waveguides at millimeter wavelengths. IEEE Trans. on MTT, MTT-27, No. 1: 31 - 37; 1979 January.

5. Hansen, R. C. "Aperture Theory," Microwave Scanning Antennas, Vol. 1., New York, NY: Academic Press; 1964.

6. Daywitt, W. C. Design and error analysis for the WR10 thermal noise standard. Nat. Bur. Stand. (U.S.) Tech. Note 1071, 1983 December.

7. Kerns, D. M. Plane-wave scattering-matrix theory of antennas and antenna-antenna interactions. Nat. Bur. Stand. (U.S.) Monogr. 162; 1981 June.

8. IEEE standard definitions of terms for antennas. IEEE Std. 145-1973.

9. The modern geometrical theory of diffraction. Vol. 1, Electro-Science Laboratory, The Ohio State University; 1982.

10. Benson, F. A. Waveguide attenuation and its correlation with surface roughness. Proc. IEE, 100, Part III: 85 -90; 1953 March.

11. Allison, J; Benson, F. A. Surface roughness and attenuation of precision-drawn, chemically polished, electropolished, electroplated and electroformed waveguides. Proc. IEE, 102B: 251 - 259; 1955 March.

12. Allis, W. P.; Herlin, M. A. Thermodynamics and statistical mechanics. New York, NY: McGraw-Hill Book Company, Inc.; 1952.

13. Terzuoli, A. J., Jr.; Peters, L., Jr. VSWR properties of E-plane dihedral corrugated horns. IEEE Trans. on A & P, AP-26, No. 2: 236 - 239; 1978 March.

14. Burnside, W. D.; Chuang, C. W. An aperture-matched horn design. IEEE Trans. on A & P, AP-30, No. 4: 790 - 796; 1982 July.

15. Jull, E. V. Reflection from the aperture of a long E-plane sectoral horn. IEEE Trans. on A & P, AP-20, No. 1: 62 - 68; 1972 January.

16. Braun, E. H. Some data for the design of electromagnetic horns. IEEE Trans. on A & P, AP-4: 29 - 31; 1956 January.

17. Ko, H. C. Antenna temperature and the temperature of electromagnetic radiation. IEEE Trans. on A & P, AP-12: 126 - 127; 1964 January.

18. Jacobsen, R. T.; Stewart, R. B.; McCarty, R. D.; Hanley, H. J. M. Thermophysical properties of nitrogen from the fusion line to 3500 R (1944 K) for pressures to 150,000 PSIA (10343 x 10^5 N/m^2). Nat. Bur. Stand. (U.S.) Tech. Note 648; 1973 December.

19. Weidman, M. WR-10 single six-port measurement system. Nat. Bur. Stand. (U.S.) NBSIR 81-1650; 1981 September.